Deep Q-Learning for Ramp Metering

Abhinav Sunderrajan, David Eckhoff, Suraj Nair, Wentong Cai, and Alois Knoll,

***Abstract*—Ramp metering, i.e., controlling the on-ramps for expressways with traffic lights, is an effective measure to reduce the disruption of the mainline flow caused by merging vehicles. Finding a traffic light program that balances delays for vehicles on the ramps and on the expressway, however, is a challenging task. To this end, we explore the possibility of employing a Deep Reinforcement Learning (DRL) solution, namely *Deep Q-Learning*, to control the traffic lights on the ramps. To the best of our knowledge, this is the first work to use neural networks for state space approximation in a reinforcement learning setting for traffic flow optimization. Our simulation results show that our approach is effective in reducing the delay experienced by the vehicles. The simulation results also show that our DRL-based approach achieves results comparable with a widely deployed ramp metering algorithm and that it can even outperform it in dynamic and high traffic volume scenarios.**

***Index Terms*—Ramp Metering, reinforcement learning, deep Q-learning, traffic light control.**

I. Introduction

The problem of traffic flow optimization has been receiving enormous interest over the last decades given the rapid increase in the number of daily trips in mega-cities around the world and constraints in terms of building new infrastructure. The increased availability of several traffic related data-streams from various sources such as smart phones, vehicles and sensors further opens possibilities for potential Advanced Traffic Information and Management Systems (ATMS).

One challenge in this regard is the traffic flow optimization on expressways, in particular the merging traffic flows from on-ramps entering the expressway. The goal is to control the flow of vehicles along the ramps to minimize the turbulence and disruption of the mainline flow. A common method to address this problem is *ramp metering*, that is, traffic light controlled on-ramps. Some of the most widely deployed ramp metering strategies are ALINEA [1], METALINE [2], SWARM [3] and HERO [4]. Finding an optimal traffic light program in order to reduce waiting times for merging vehicles while at the same time minimizing the impact on expressway traffic, however, is a challenging task.

To this end, we deploy machine learning techniques, in particular reinforcement learning (RL) to find the optimal signal changes for the ramp traffic lights. One of these techniques is the model-free Q-learning, which was shown to be a promising approach to optimize traffic flows [5]. However, the fact that Q-learning requires a finite set of states reduced its applicability for large scenarios. The problem of a large and continuous state space for traffic systems was solved in [6], [7] (discussed in Section II) by quantizing it. Quantization of state space is challenging for traffic which is a complex non-linear stochastic system. As discussed in [8] the problems associated with quantizing state space can be avoided by the use of artificial neural networks (ANN). Up until recently the use of non-linear function approximators such as ANN caused it to diverge and thus hinder learning.

Recently the authors of [9] introduced *Deep Q-Learning* which mastered difficult control policies for playing computer video games from raw pixel data. The authors employ a technique called *experience replay* (explained later) to successfully train the weights of a *convolutional neural network* used for state-space approximation without divergence issues. In this article, we show how the problem of optimizing ramp metering can be tackled by applying deep Q-learning to train on-ramp traffic lights. Our primary objective in this context is to reduce the overall delay experienced by vehicles on both the expressway as well as the on- and off-ramps. The contributions of this paper are:

- We propose an adaptive and live ramp-metering strategy using deep Q-learning.
- We show the applicability of our method by simulating a real-world expressway in the city of Singapore and quantify the benefit in terms of reduced delay.
- We evaluate and establish the ability of the algorithm to generalize and achieve good performance despite random flow rates along the roads and stochastic fluctuations in traffic flow.
- We demonstrate the potentials of deep Q-learning for ramp metering by comparing with ALINEA which serves as benchmark.

The remainder of this article is organized as follows: We review literature onramp metering and approaches towards using reinforcement learning for traffic flow control and optimization in Section II. In Section III we present the system model used for our approach, followed by an explanation of the deployed deep Q-learning approach (Section IV). In Section V the results of our simulation study are shown before concluding the paper in Section VI.

II. Related Work

In this section we describe ramp metering as traffic flow control/optimization strategy before delving into RL-based approaches for traffic flow optimization. Ramp metering strategies are classified into two types, *fixed-time* and *reactive* [10]. The fixed-time strategy is based on historical data pertaining to flow rates along the on-ramps and the expressway at different times of the day. The main drawback of the fixed-time strategy is that their settings are based on historic rather than real-time data. It does not take into account the varying nature of traffic demand and the occurrence of events such as accidents and road blocks which could cause massive congestions.

Reactive ramp metering strategies aim to optimize the flow of traffic based on real-time measurements. Reactive ramp metering is classified into two types: *Local Ramp Metering* (e.g. ALINEA) and *Multivariable Regulator Strategies* (e.g. METALINE) [10]. The former makes use of measurements in the vicinity of an on-ramp to regulate the flow on the ramp. The control strategy applied for an on-ramp is independent of the measurements and controls applied in other on-ramps in the vicinity. While the latter makes use of the system wide measurements to simultaneously regulate traffic flow along all on-ramps. A review on several recent ramp metering strategies can be found in [11].

In this work we use ALINEA, a local ramp metering strategy as a benchmark for evaluating our approach. Field trials of ALINEA have shown it to be superior compared to other local ramp metering strategies and the no control case. Field trials comparing the performance of ALINEA and the more sophisticated METALINE (based on advanced control strategies such as linear-quadratic control) [2] show that the former performs as the latter except in cases of events such as accidents due to more comprehensive measurements. The implementation of ALINEA is as follows

$$y^{\text{on}}_{\text{ramp}}(k) = y^{\text{on}}_{\text{ramp}}(k-1) + K_R(\rho^{\text{crit}}_{\text{out}}(k-1) - \rho_{\text{out}}(k-1)) \quad (1)$$

where $y^{\text{on}}_{\text{ramp}}(k)$ is the on-ramp flow at time-step k, $\rho^{\text{crit}}_{\text{out}}(k-1)$ and $\rho_{\text{out}}(k-1)$ represents the critical and the current densities of the downstream cell. $K_R > 0$ is the constant regulator parameter. ALINEA thus decreases the ramp flow by adjusting the traffic light when the density of the downstream cell is greater than its critical density.

One of the first papers to employ reinforcement learning for controlling traffic is [5]. The authors employ the classic Q-learning algorithm for traffic signal control of a single intersection. They employ a more sophisticated version of a *Q-table* (explained in Section IV) for storing and updating the Q-values for each state action pair. However, it does not scale for large traffic scenarios, because Q-learning works on finite states to determine the next action, in this case, changing a traffic light signal. Quantizing the state space is challenging as there exists no general-purpose approach and scenario-specific knowledge is required.

Prashanth et al. [7] solve the problem of high-dimensional state-action spaces using a linear function approximation technique. The authors use a variant of Q-learning to reduce the queue lengths of vehicles waiting at an intersection which also represents the state of the traffic network simulated. To reduce the number of states, the authors parameterize the vehicle queue lengths. For instance queues with length less than $L1$ units are considered to be *low* while queues with lengths in between thresholds $L1$ and $L2$ units are classified as *medium*. Queue lengths exceeding $L2$ units are classified as high. This work showed that RL with function-approximation is a better approach for traffic signal control in comparison to other strategies such as fixed timing and counting number of vehicles waiting at each lane for terms of reducing delay.

The authors of [6] implement a Q-learning approach to reduce traffic delay experienced in an urban street network by simulating peak hour traffic in the central business district of Singapore. The authors discretized the state space based on the data from vehicle queue and flow (at intersections) into 9 possible states to construct a Q-table. The authors were able to achieve a near 12% improvement in reducing traffic delay compared to existing benchmark solutions such as GLIDE [12] (a modified version of SCATS used in Singapore).

As mentioned previously, we use an ANN with two hidden layers for state space generalization. To our knowledge this is the first work to use deep Q-learning for controlling the flow of vehicle along on-ramps using ramp metering.

III. System Model

In this section we describe our macroscopic traffic flow simulation. Description of the traffic simulator will set up the description of traffic state, action and the reward for the RL agent described in the next section.

The traffic simulator in this work is a faster than wall-clock time macroscopic simulation which is based on the stochastic variant of the Cell transmission model [13] and METANET [14]. The cell network $\mathbb{C}$ is comprised of n cells. At each time-step, $k = 0, 1, ...K$ (where K is the time horizon) the state of all cells are updated. The discrete event simulation time-step used for this simulator is a constant, $k = 4$ seconds in all the experiments.

The state of a cell $c_i \in \mathbb{C}$ at each time-step k is determined by the concept of *sending* $S_i(k)$ and *receiving potentials* $R_i(k)$. $S_i(k)$ and $R_i(k)$ represent the number of vehicles cell c_i can send and receive at time-step k. The mean and standard deviation of speed for a cell c_i are denoted by $v_i(k)$ and $v^{\text{sd}}_i(k)$ respectively. The number of vehicles in a cell c_i at time-step k is given by $N_i(k)$. While $N^{\max}_i(k)$ represents the maximum number of vehicles that can be accommodated in cell c_i given an average speed of $v_i(k)$. $N^{\max}_i(k)$ is given by

$$N^{\max}_i(k) = \frac{l_i \cdot \lambda_i}{T_{\text{gap}} \cdot v_i(k) + L_{\text{eff}}} \quad (2)$$

where L_{eff} is the *effective* vehicle length while T_{gap} represents the safe time gap. The length of cell c_i is denoted by l_i which is a variable and subject to the constraint $l_i \geq V^i_0 \cdot T$. Where V^i_0 is the constant free-flow speed for the cell. This constraint ensures that no vehicle can enter and exit a cell within one time-step. The number of lanes in cell c_i corresponding to the associated road-link is denoted by λ_i. Finally $y_i(k)$ represents the number of vehicles that exit a cell c_i during the time interval k through $k + 1$, given the average speed in the cell during this time interval is $v_i(k)$.

The cells constituting the cell network $\mathbb{C}$ are classified into five different types as shown in Figure 1. Note that this is an illustrative network and not the real-world expressway (see Section V-A) simulated for the experiments. The *Merging* cells are associated with the parameter *merge priority* $\mu \in [0.0, 1.0]$ which controls the proportion of vehicles that moves to the next cell in a given time-step. The *Source* and *Sink* cells are not

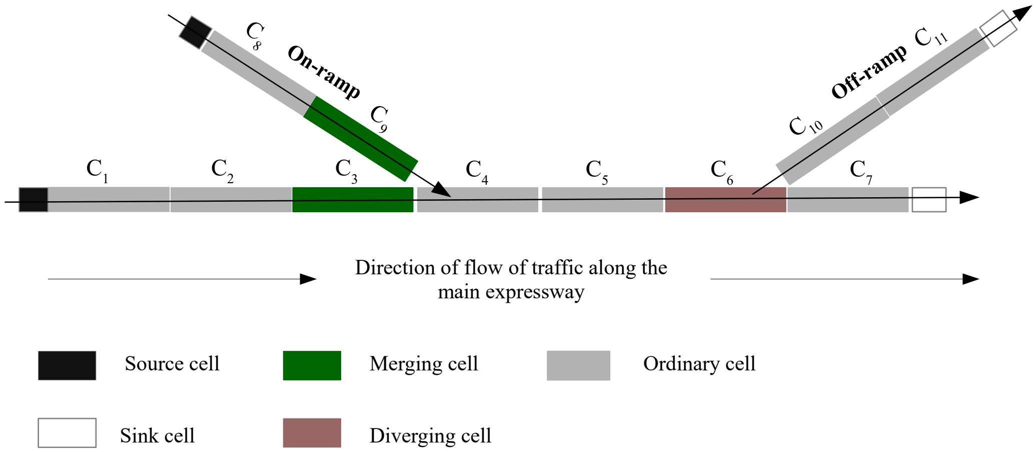

Fig. 1: An illustrative cell network.

physically related to any of the road links but are effectively *ghost cells*. The former injects vehicles into the simulation while the vehicles exit the simulation through the latter. Note that the inter-arrival rates of vehicles at all source cells are kept constant during simulation time horizon of K time-steps. A *Diverging* cell is associated with the turn ratios $\tau \in [0.0, 1.0]$, representing the proportion of vehicles exiting the expressway through off-ramps and those continuing to traverse along the expressway. Cells C_3 and C_9 are considered *predecessors* of cell C_4 while cells C_{10} and C_7 are considered *successors* of cell C_6.

Refer to the technical report [15] for details on the algorithm and equations governing the model of this stochastic traffic simulation. Stochastic noise is added to the function decreasing the mean-flow speed of each cell which results in the creation of spontaneous *phantom jams* and shock waves as occurring in real life.

IV. Deep Q-learning for ramp metering

In this paper we use the variant of Q-learning called *Deep Q-learning* introduced in [9]. Q-learning [16] is an RL algorithm which is known to converge to the optimal policy. Q-learning is characterized by a set of states $\mathbf{S}$ and actions $\mathbf{A}$. Q-learning is a *model free* technique which learns the action-value (also known as Q) function represented by $Q^*(s,a)$ providing the expected utility of taking an action $a \in \mathbf{A}$ in given state $s \in \mathbf{S}$ of the environment and then following the optimal policy there afterwards.

The basic implementation of Q-learning uses Q-tables to store the action-values. Each row represents the state $s \in \mathbf{S}$ while each column represents the actions $a \in \mathbf{A}$. This approach is not feasible for many real-world control scenarios consisting of hundreds of millions of states. Consider the case of traffic where the state space is continuous and hence infinite. This problem is usually overcome by the use of *function approximators* for the action value function represented as $Q(s,a;\theta) \approx Q(s,a)$. The most common function approximators are linear in nature. For stochastic non-linear systems such as traffic, a non-linear function approximator such as neural network can be used. In the case of neural networks θ represents the weights of the underlying neurons.

For this work, we are inspired by the recent successes of Mnih et.al [9] in effectively training convolutional neural networks (for non-linear function approximation) to achieve human level performance in playing several video games. The ANN used in our work for generalizing the state space, enables the ramp metering controller to take the appropriate control action at the on-ramps in expressway sections. The controller for operating the ramp meters is referred to as the DRL-agent henceforth. As pointed out in [9] the DRL algorithm uses a biologically inspired technique called *experience replay* for *off-policy* learning where the agent takes an action $a = max_a Q(s,a;\theta)$ with probability $1-\epsilon$ and a random action with probability ϵ ensuring adequate exploration of the state space.

In this section we describe the Markov decision process (MDP) for reducing traffic delay using ramp metering. The goal of the DRL-agent is to minimize the net discounted delay experienced by all vehicles in all cells over a fixed time horizon of K time-steps. The DRL-agent achieves this by learning a policy to determine the appropriate traffic light configuration for all controllable on-ramps depending upon the state in the simulator. The simulator also provides rewards (discussed subsequently) which is used by the DRL-agent to determine the utility of an action taken.

A. Traffic State

The state of the simulator at time-step k is defined in terms of state of each cell $c_i \in \mathbb{C}$ (except source and sink cells) given by $\frac{n_i(k)}{N_i^{\max}(k)}$. This represents the ratio of the number of vehicles in c_i to the maximum number of vehicles that can be accommodated in c_i at time-step k.

B. Reward Computation

The total delay D_{total} over K time-steps is given by

$$D_{\text{total}} = \sum_{k=0}^{K} \sum_{i=0}^{|\mathbb{C}|} d_i(k) \tag{3}$$

where $d_i(k)$ is the delay experienced by cell $c_i \in \mathbb{C}$ at time-step k. The delay $d_i(k)$ is given by

$$d_i(k) = min\Big(0, y_i^{\text{free}}(k) - y_i(k)\Big) \tag{4}$$

The parameter $y_i^{\text{free}}(k)$ represents the number of vehicles that would have exited cell c_i during time-step k if $v_i(k) = V_i^0$. Equation 4 thus represents the number of vehicles affected due to congestion in the cell network in all cells $c_i \in \mathbb{C}$ at time-step
k.

The reward r_{k+1} at the end of time-step k is given by

$$r_{k+1} = \begin{cases} \frac{(D_{\text{total}}^{\text{noRM}} - D_{\text{total}}^{\text{RM}})}{D_{\text{total}}^{\text{noRM}}}, & \text{if } k = K \\ 0, & \text{otherwise} \end{cases} \tag{5}$$

$D_{\text{total}}^{\text{noRM}}$ represents the total delay when no ramp metering is employed while $D_{\text{total}}^{\text{RM}}$ represents the total delay experienced over K time-steps when ramp metering is employed using the policy determined by the ANN. The DRL-agent thus tries to learn a ramp metering policy which tries to minimize the total delay experienced by all vehicles over a time horizon of K time-steps in comparison to baseline policy of no ramp metering control. The reward at the end of terminal time-step K is clipped to be in range $-1.0 \leq r_{K+1} \leq 1.0$ as suggested in [9].

C. Actions and Setup for Reinforcement Learning

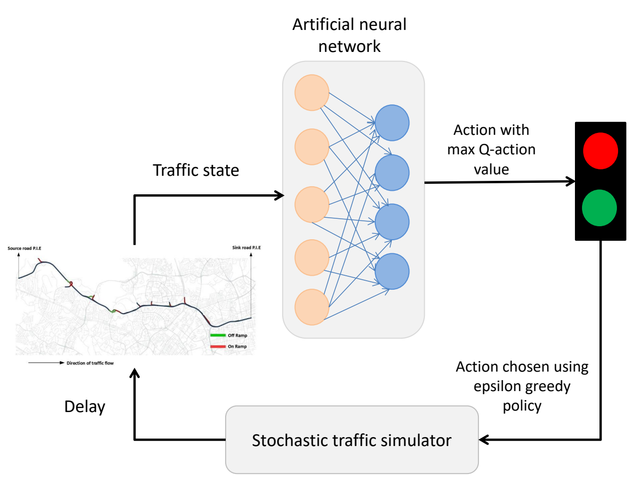

Fig. 2: Deep Q-learning for ramp metering.

Figure 2 shows the setup for adaptive ramp metering control using deep Q-learning. In our experiments the minimum phase time for each ramp meter is 12 seconds, i.e. 3 simulation time-steps. Given that the light at each controllable on-ramp can either be red or green, the number of actions that can be taken at time-step k is 2^{Ψ} where Ψ denotes the number of controllable on-ramps.

After 3 simulation time-steps the traffic simulator gives the state of each of cell $c_i \in \mathbb{C}$ (excluding source and sink cells) as an input to the ANN. As mentioned previously, traffic state at time-step k is given by the ratio of number of vehicles to the maximum number of vehicles that an be accommodated in a cell (for the current traffic speed) for all cells belonging to the cell network $\mathbb{C}$. The state space is infinite since the ratios $\frac{n_i(k)}{N_i^{\max}(k)}$ (representing the state) for all cells are real valued and continuous. The output layer of the ANN consist of 2^{Ψ} neurons representing the number of actions that the DRL-agent can make. The action a is chosen from ANN output based on the ϵ greedy (see lines 9 through 12 of Algorithm 1) policy. The traffic light combination corresponding to the output of the ANN is given as an input to the traffic simulator which computes the next state and the delay incurred in subsequent

Algorithm 1 Deep Q-learning for adaptive ramp metering control.

```
1: Initialize replay memory 𝕄 of size 32.
2: Initialize the neural network (action-value function) Q
   with weights Θ.
3: Initialize the target action-value function (another neural
   network) Q̄ for generating t_j with weights Θ̄ ← Θ.
4: repeat
5:     Set random flow rates at all source cells.
6:     Warm up traffic simulator.
7:     for k = 0, K do
8:         Get the state s_k from the cell network in simulator.
9:         if random_double < ε then
10:            Select random action a_t
11:        else
12:            Select action a_k = argmax_a Q(s_k, a; θ)
13:        Observe the reward r_{k+1} for the action a_k
               and the new cell state s_{k+1}
14:        Create transition tuple T = (s_k, a_k, r_{k+1}, s_{k+1})
15:        if size(𝕄) < N then
16:            Add T to memory 𝕄
17:        else
18:            replace first element in 𝕄 with the tuple T
19:            Sample random mini-batch 𝔹 from 𝕄
20:            for each T ∈ 𝔹 do
21:                if (j + 1) < K then
22:                    t_j = r_j + γ · max_a(Q̄(s_{j+1}, a_{j+1}; Θ̄))
23:                else
24:                    t_j = r_j
25:                Use (t_j − Q(s_j, a_j; Θ))^2 for gradient
                       descent with respect to Θ.
26:            After C steps, reset Q̄ ← Q
27: until epoch < epoch_max
```

3 time-steps.

Considering that the DRL-agent acquires the traffic state of all cells of the expressway and controls the Ψ controllable on-ramps simultaneously, the DRL-based ramp metering is a multivariable regulator ramp metering strategy.

Refer to Algorithm 1 implementing experience replay for training the DRL-agent for ramp metering control. To perform experience replay, we store the DRL-agent's experience as a transition tuple $\mathbf{T} = (s_t, a_t, r_{t+1}, s_{t+1})$ to the replay memory data store $\mathbb{M}$. The standard RL assumption that future rewards are discounted by a constant factor $\gamma = 0.99$ is made. See [16] for more details regarding discounting future rewards during Q-learning. During the training process, random mini batches $\mathbb{B}$ of size 32 are sampled from $\mathbb{M}$. Experience replay thus avoids the pitfall of learning from consecutive samples which are strongly correlated. As suggested in [9], two artificial neural networks are used to improve the stability of the learning process. The ANN Q with weights Θ represents the action-value function Q while the ANN $\bar{Q}$ with weights $\bar{\Theta}$ generates the Q-learning targets t_j (see line 22 of Algorithm-1). The weights of the ANN $\bar{Q}$ are replaced with those of Q every $C = 50$ steps. Note that epoch refers to one forward pass and one backward pass of the neural network over the mini batch $\mathbb{M}$.

V. Experiments

In this section we begin with a description of the hyper-parameters used for training the DRL-agent. Description of the experimental setup, the training process of the DRL-agent, evaluation of the DRL-agent's performance followed by a brief discussion of the results of evaluation. The details of the hyper-parameters used for training the DRL-agent (as described in Algorithm 1) are shown in Table I. The ANN consists of two hidden layers with sizes equal to 200 and 150 neurons each. The size of the input layer is equal to the number of physical cells in the simulated expressway section. The size of the output layer corresponds to the number of actions that the DRL-agent can take at each state. The size of the output layer is thus 2^{Ψ} as explained previously. The hidden layers of the ANN employ *leaky rectified linear unit* (ReLU) as the activation function for each neuron. The output layer uses the *identity* activation function which is commonly used for regression problems.

A. The Simulated Environment

For the experiments in this report, we simulate a 13 km stretch of P.I.E. (Pan Island Expressway) in central Singapore (Figure 3) with all on and off-ramps. The on-ramps and the first P.I.E. link are sources, while all off-ramps and the last link on P.I.E. are sinks. Refer to the Table II for the location of all on/off-ramps starting from the beginning of the first road-segment on P.I.E. The average distance between two on-ramps is around 565 m along this stretch of P.I.E. The turn ratios for all off-ramps is kept constant at $\tau = 0.25$. This implies that 25% of all vehicles exit at a given off-ramp while the remaining 75% of the vehicles continue to travel on the main expressway. The number of lanes in the simulated stretch of the expressway varies between 3 and 6. The total number of cells in the cell network for the expressway section simulated (including on/off-ramps and excluding the source and link cells) is 212.

Fig. 3: Simulated 13 km section of P.I.E. (Singapore) and location of all on/off-ramps.

B. Traffic Scenario

Table II lists the range of mean in-flow rates in vehicles/hour for all source links. The mean flow rates for an episode of the simulation is picked randomly within the specified range and kept constant during the simulated time horizon for all experiments (training as well as evaluation) in this paper. Notice that the flow of vehicles into the expressway along all $\Psi = 4$ controllable on-ramps is less than that of the ones which do not have ramp meters.

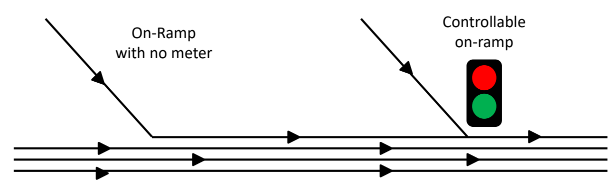

Fig. 4: Structure of on-ramps in the traffic simulation.

Figure 4 illustrates the difference between a controllable on-ramp and an ordinary one with no traffic light. Vehicles entering the P.I.E along an on-ramp with no ramp meter cause lesser disruption to the main line flow compared to the on-ramps with meters due to the presence of an extra lane.

C. Training

The ANN is trained to determine the appropriate action when the traffic state from all the cell network (except the source and sink) are given to it as inputs. The output of the ANN is used to determine the actions based on the ϵ greedy strategy. Figure 5 plots the action-value function Q which provides an estimate of how much discounted reward a DRL-agent can get by taking an action a in a state s and following the policy from there onwards. As suggested in [9] we collect a fixed set of states before training starts to track the average

TABLE I: Hyper-parameters used for deep Q-learning.

Hyper Parameter	Value	Description
Number of hidden layers	2	The number of hidden layers in the neural network used for Deep Q-learning. The first hidden layer consists of 200 neurons while the second hidden layer is composed of 150 neurons.
Learning rate	0.00025	Learning rate used by the RMSProp algorithm.
Discount factor	0.98	Discount factor used in Q-learning update.
Replay memory size	1500000	Stochastic gradient descent updates are sampled from this number of recent $(s_t, a_t, r_{t+}, s_{t+1})$ tuples stored in memory.
Mini batch size	32	The batch size used by the stochastic Gradient descent (SGD) update of neural network weights.
RMS decay	0.95	Gradient momentum used by the RMSProp algorithm.
Initial exploration	1.0	The initial ϵ in the ϵ greedy evaluation.
Final exploration	0.05	The final ϵ in the ϵ greedy evaluation.
Target network update frequency	100	The frequency with which target network (in number of steps) is evaluated.

TABLE II: Mean flow rates at all on-ramps.

Distance (m)	Ramp type	Flow (vehicles/hour)
0.0	First P.I.E. link	3600 - 4000
583.98	On-ramp	1100-1600
2489.87	On-ramp	1100-1600
4071.9	Controllable on-ramp	800 - 1100
5531.18	On-ramp	1100-1600
5965.29	On-ramp	1100-1600
7025.15	On-ramp	1100-1600
7658.4	Controllable on-ramp	800 - 1100
8554.28	Controllable on-ramp	800 - 1100
9591.84	On-ramp	1100-1600
11286.2	On-ramp	1100-1600
11286.2	Controllable on-ramp	800 - 1100

of the maximum predicted action-value for these states. A smooth increase in the Q-value which stabilizes after epoch 450 suggests that deep Q-learning is able to train our ANN using stochastic gradient descent in a stable manner despite the lack of any theoretical convergence guarantees. For Figure 5, the average flow rates for all sources were randomly sampled in the ranges specified in Table II. As previously stated, the

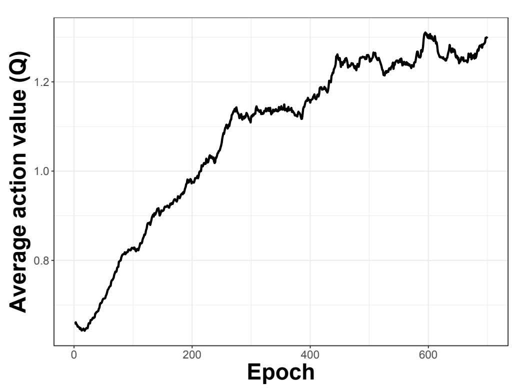

Fig. 5: Average action-value.

mean inter-arrival times (and thus flow rates) for all source links/cells are kept constant for an episode of K time-steps.

D. Evaluation

As explained in Section IV, the goal of our reinforcement learning algorithm is to determine a ramp-meter policy which tries to reduce the total delay D_{total} (in comparison to the no control case) experienced by all vehicles over a time horizon of $k = K$ time-steps. At the end of the training over 500 epochs, we sampled random flow rates (for the source cells) within the ranges specified in Table II and conducted 800 trials to compare the delays experienced by the vehicles with and without ramp metering. The ramp metering policy is determined by the trained ANN which uses the traffic state as input to determine the appropriate traffic lights for the 4 controllable on-ramps. The ANN chooses the action corresponding to the maximum Q-Value for each state with a probability of 0.999 and chooses a random action otherwise. This is done in order to avoid over fitting.

TABLE III: Mean traffic density level.

Traffic density level	Density range (veh/km/lane)	Traffic State
1	[30, 34]	Synchronized flow
2	(34-38]	Synchronized flow
3	(38-42]	Synchronized flow
4	(42-46]	Congested

As stated earlier, we implemented the local ramp metering strategy of ALINEA(Equation 1). We chose the constant regulator parameter $K_R = 70.0$ based on [2]. Figure 6a compares the percentage improvement in the overall delay (for all roads including the on/off ramps) for the ramp metering policy determined by the DRL-agent and that of ALINEA over the no ramp metering case for different mean traffic-density levels ranging from synchronized flow to congested (see Table III). The number of trials in each traffic density level numbers 200 for ALINEA and DRL. Note that the simulation seeds were changed for each of the 800 trials (200 in each traffic density category) to take into account the stochasticity associated with the traffic flow simulator. The overall median

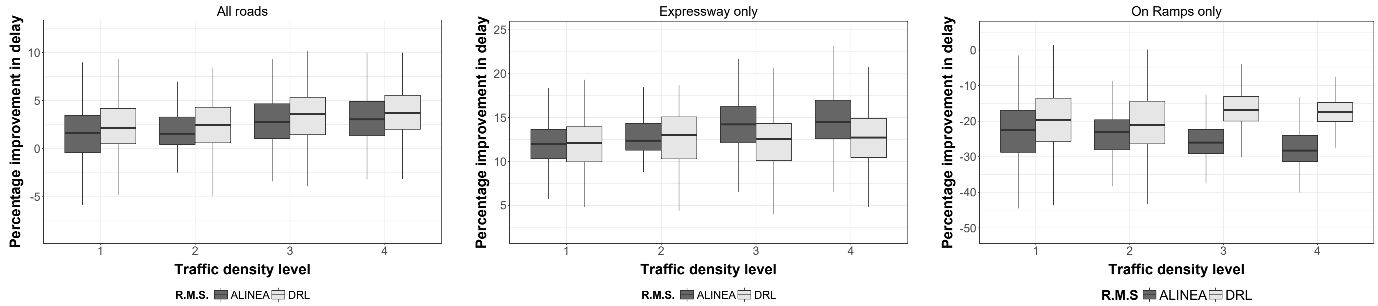

(a) For all cells including on and off ramps

(b) For the cells constituting expressway section only

(c) For the cells constituting the on-ramps only

Fig. 6: Percentage of delay reduction for the two ramp metering strategies (RMS) DRL and ALINEA.

improvement for the DRL-based ramp metering strategy is comparatively better than ALINEA.

Figure 6 shows the results of our simulation study in terms of relative delay experienced by the vehicles compared to an approach where no ramp metering is applied. We observe that the overall delay reduction (Figure 6a) is similar for ALINEA and DRL, with indications of DRL performing slightly better. Figure 6b compares the delay experienced over the main-line expressway cells only between ALINEA and DRL. The results indicate that the median delay experienced over the expressway is lower for ALINEA especially at higher traffic density levels of 3 and 4. The reason for the delay benefit over the expressway becomes apparent in Figure 6c where the median delay for the on-ramps is higher for ALINEA (compared to DRL) for the traffic density level 3 and 4. In summary, ALINEA trades a higher delay on the on-ramps to achieve better performance on the expressways. However, this leads to an overall delay for all vehicles that is higher than what we observe using our DRL approach, where the delay of each car is treated equally. We can tune the algorithm to favor the reduction of delay of the expressway cells over those on the on/off-ramps by weighting the expressway cell(s) delay by a factor $f > 1.0$. This will come at the cost of increased delay along the on-ramps potentially causing spillovers to the urban street network which we want to avoid.

Figures 7 plots the variation of delay for all cells as the average traffic density (in veh/km/lane) is gradually increased from levels 1 through 4 and beyond over 1800 seconds for different ramp metering strategies. Note that the results of Figures 7 are averaged over 5 different trials of the simulator with varying simulation seeds to account for the model stochasticity. The simulated scenario represents a typical rush hour where the traffic state goes from synchronized flow to congested in a short period of time. We observe that the performance of both ALINEA and DRL for overall delay are comparable for densities up until 45 veh/km/lane corresponding to a synchronized traffic flow regime. DRL actually performs better than ALINEA when the traffic conditions are congested for densities beyond 45 veh/km/lane by adaptively varying the traffic lights at all 4 controllable on-ramps.

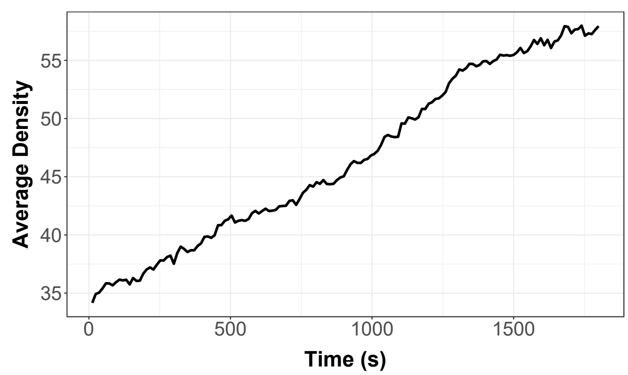

(a) Average traffic density in the rush hour scenario

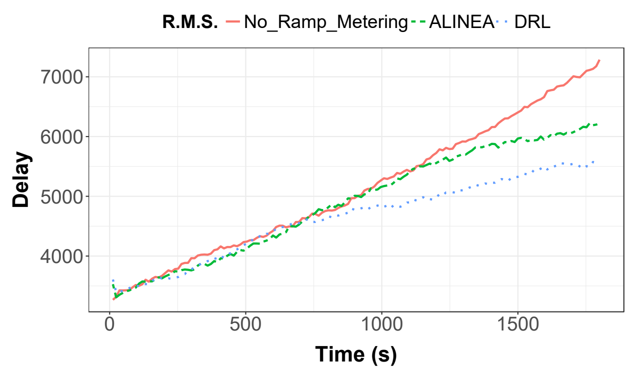

(b) Delay experienced by all vehicles in the simulation

Fig. 7: Overall delay for different ramp metering strategies as traffic density is gradually increased over 1800 seconds.

E. Discussion Of Results

The evaluation of the results shows that deep Q-learning is able to learn a policy to minimize the overall and mainline expressway delays over a simulated time horizon of K time-steps. The results also show that deep Q-learning has generalized well given random traffic flows at the sources and the inherent stochasticity in the simulator which causes spontaneous emergence of jams. Encouragingly, the performance of DRL is comparable to ALINEA, a widely deployed and successful ramp metering strategy for synchronized traffic flow conditions. Our simulations show that DRL performs better than ALINEA when the traffic flow regime is congested.

The objective of this paper is to show that deep Q-learning can be used to determine model-free policies for ramp metering despite the inherent randomness in traffic systems. There are reasonable chances that the policy determined may not be optimal due to the lack of any theoretical guarantees since ANN is employed for function approximation.

VI. Conclusion and Future Work

In this paper, we explored the possibility of applying deep Q-learning for ramp metering and showed that it has the potential for true adaptive real-time traffic control under uncertainty. Deep Q-learning as demonstrated by the recent successes in training computers to pay video games helps us overcome the disadvantages associated with quantizing the near infinite state space.

We simulated a real-word expressway in the city-state of Singapore using a cell based traffic flow model, which offers fast and efficient performance when used in computer simulations at a macroscopic scale. This efficiency allowed us to run the high number of iterations required for deep Q-learning to converge. We found that for different traffic densities, our approach is indeed feasible and produces similar results as the widely used local ramp metering strategy ALINEA. In fact, under dynamic traffic conditions, e.g., at the beginning of the rush hour, our approach outperformed ALINEA yielding a lower delay for all vehicles.

This work has the potential to be extended for other optimal traffic control strategies in urban environments through adaptive traffic signal timings. Other control strategies that can be investigated for efficacy include variable speed limits, congestion aware routing and traffic signal timing optimization. Additionally, our approach can be altered using different reward functions, e.g., weighing delays on-ramps or expressways differently.

Acknowledgment

This work was financially supported by the Singapore National Research Foundation under its Campus for Research Excellence And Technological Enterprise (CREATE) programme.

TABLE IV: List of important symbols used in the paper.

Symbol	Explanation
k	Constant simulator time-step.
c_i	A cell belonging to the cell network $\mathbb{C}$.
l_i	Length of c_i.
λ_i	Number of lanes in c_i.
$v_i(k)$	The average speed of vehicles in c_i at k.
$\rho_i(k)$	The vehicle density in c_i at k.
$n_i(k)$	Number of vehicles in c_i at k.
$N_i^{\max}(k)$	Maximum number of vehicles that can be accommodated in c_i at k.
V_i^0	The free-flow velocity of c_i.
$y_i(k)$	The outflow from c_i during k.
y_i^{free}	The outflow from c_i during k given $v_i(k) = V_i^0$.
$d_i(k)$	Delay experienced in c_i during k.
D_{total}	Sum of total delay experienced by all cells over the entire time horizon.
$S_i(k)$	The sending potential of c_i at k.
$R_i(k)$	The receiving potential of c_i at k.
$y_{\text{ramp}}^{\text{on}}(k)$	Flow from the on-ramp on to the expressway.
K_R	ALINEA constant regulator parameter.
$Q(s,a)$	Action value or Q function.
s	A state $s \in \mathbf{S}$ of the environment.
a	An action $a \in \mathbf{A}$ the DRL-agent can make.
$Q(s,a;\theta)$	A Q function using a nonlinear function approximator such as an ANN. Here θ represents the weights of an ANN used for state space approximation.
Ψ	Number of controllable on-ramps.
γ	The discount factor for future rewards

References

[1] M. Papageorgiou, H. Hadj-Salem, and J.-M. Blosseville, "Alinea: A local feedback control law for on-ramp metering," *Transportation Research Record*, no. 1320, 1991.

[2] M. Papageorgiou, H. Hadj-Salem, and F. Middelham, "Alinea local ramp metering: Summary of field results," *Transportation Research Record: Journal of the Transportation Research Board*, no. 1603, pp. 90–98, 1997.

[3] G. Paesani, J. Kerr, P. Perovich, and F. Khosravi, "System wide adaptive ramp metering (swarm)," in *Merging the Transportation and Communications Revolutions. Abstracts for ITS America Seventh Annual Meeting and Exposition*, 1997.

[4] I. Papamichail, M. Papageorgiou, V. Vong, and J. Gaffney, "Heuristic ramp-metering coordination strategy implemented at monash freeway, australia," *Transportation Research Record: Journal of the Transportation Research Board*, no. 2178, pp. 10–20, 2010.

[5] B. Abdulhai, R. Pringle, and G. J. Karakoulas, "Reinforcement learning for true adaptive traffic signal control," *Journal of Transportation Engineering*, vol. 129, no. 3, pp. 278–285, 2003.

[6] P. Balaji, X. German, and D. Srinivasan, "Urban traffic signal control using reinforcement learning agents," *IET Intelligent Transport Systems*, vol. 4, no. 3, pp. 177–188, 2010.

[7] L. Prashanth and S. Bhatnagar, "Reinforcement learning with function approximation for traffic signal control," *IEEE Transactions on Intelligent Transportation Systems*, vol. 12, no. 2, pp. 412–421, 2011.

[8] J. C. Santamaría, R. S. Sutton, and A. Ram, "Experiments with reinforcement learning in problems with continuous state and action spaces," *Adaptive behavior*, vol. 6, no. 2, pp. 163–217, 1997.

[9] V. Mnih, K. Kavukcuoglu, D. Silver, A. A. Rusu, J. Veness, M. G. Bellemare, A. Graves, M. Riedmiller, A. K. Fidjeland, G. Ostrovski *et al.*, "Human-level control through deep reinforcement learning," *Nature*, vol. 518, no. 7540, pp. 529–533, 2015.

[10] M. Papageorgiou, C. Diakaki, V. Dinopoulou, A. Kotsialos, and Y. Wang, "Review of road traffic control strategies," *Proceedings of the IEEE*, vol. 91, no. 12, pp. 2043–2067, 2003.

[11] K. Shaaban, M. A. Khan, and R. Hamila, "Literature review of advancements in adaptive ramp metering," *Procedia Computer Science*, vol. 83, pp. 203–211, 2016.

[12] C. K. Keong, "The glide systemsingapore's urban traffic control system," *Transport reviews*, vol. 13, no. 4, pp. 295–305, 1993.

[13] R. Boel and L. Mihaylova, "A compositional stochastic model for real time freeway traffic simulation," *Transportation Research Part B: Methodological*, vol. 40, no. 4, pp. 319–334, 2006.

[14] A. Kotsialos, M. Papageorgiou, C. Diakaki, Y. Pavlis, and F. Middelham, "Traffic flow modeling of large-scale motorway networks using the macroscopic modeling tool metanet," *Intelligent Transportation Systems, IEEE Transactions on*, vol. 3, no. 4, pp. 282–292, 2002.

[15] A. Sunderrajan, V. Viswanathan, W. Cai, and A. Knoll, "Symbiotic traffic simulation framework," no. TUM-I1642, 2016. [Online]. Available: https://mediatum.ub.tum.de/?id=1325684

[16] R. S. Sutton and A. G. Barto, *Reinforcement learning: An introduction*. MIT press Cambridge, 1998, vol. 1, no. 1.